Hindawi
Advances in Materials Science and Engineering
Volume 2017, Article ID 2602953, 12 pages
https://doi.org/10.1155/2017/2602953

Research Article

Study on Mechanical Relaxations of 7075 (Al–Zn–Mg) and 2024 (Al–Cu–Mg) Alloys by Application of the Time-Temperature Superposition Principle

Jose I. Rojas,[1,2] Jorge Nicolás,[2] and Daniel Crespo[2,3]

[1]*Department of Physics, Division of Aerospace Engineering, Universitat Politècnica de Catalunya, Barcelona, Spain*
[2]*Escola d'Enginyeria de Telecomunicació i Aeroespacial de Castelldefels, Universitat Politècnica de Catalunya, c/Esteve Terradas 7, 08860 Castelldefels, Spain*
[3]*Department of Physics, Universitat Politècnica de Catalunya, Barcelona, Spain*

Correspondence should be addressed to Jose I. Rojas; josep.ignasi.rojas@upc.edu

Received 1 January 2017; Accepted 13 March 2017; Published 5 April 2017

Academic Editor: Ming-Xing Zhang

The viscoelastic response of commercial Al–Zn–Mg and Al–Cu–Mg alloys was measured with a dynamic-mechanical analyzer (DMA) as a function of the temperature (from 30 to 425°C) and the loading frequency (from 0.01 to 150 Hz). The time-temperature superposition (TTS) principle has proven to be useful in studying mechanical relaxations and obtaining master curves for amorphous materials. In this work, the TTS principle is applied to the measured viscoelastic data (i.e., the storage and loss moduli) to obtain the corresponding master curves and to analyze the mechanical relaxations responsible for the viscoelastic behavior of the studied alloys. For the storage modulus it was possible to identify a master curve for a low-temperature region (from room temperature to 150°C) and, for the storage and loss moduli, another master curve for a high-temperature region (from 320 to 375°C). These temperature regions are coincidental with the stable intervals where no phase transformations occur. The different temperature dependencies of the shift factors for the identified master curves, manifested by different values of the activation energy in the Arrhenius expressions for the shift factor, are due to the occurrence of microstructural changes and variations in the relaxation mechanisms between the mentioned temperature regions.

1. Introduction

Comprehensive research efforts have been devoted to characterizing the mechanical properties of metals. However, their viscoelastic response, a manifestation of internal friction phenomena under dynamic loading, has received much less attention. The comprehension of the underlying physics of viscoelasticity is of high interest because it enables a deeper understanding of important properties like mechanical damping and yielding [1] and because metals are subjected to dynamic loads in most of their structural applications. Indeed, fatigue is a consequence of microstructural changes induced under dynamic loading, and these phenomena must have an effect on the viscoelastic response [2], as it is also intimately linked to the microstructure [1]. Thus, the study of the viscoelastic behavior offers a different approach for analyzing the microstructure and the fatigue behavior of a material. The former has been shown in metallic glasses, for which structural relaxations, the glass transition, and crystallization processes have been studied with dynamic-mechanical analyzers (DMA) [3]. Also, the time-temperature superposition (TTS) principle has proven useful in studying the mechanical relaxations and in obtaining master curves for amorphous materials [4, 5].

In this work, a similar approach is applied to commercial 7075 (Al–Zn–Mg) and 2024 (Al–Cu–Mg) alloys. Particularly, the TTS principle is applied to experimental viscoelastic data, that is, the storage modulus E' and the loss modulus E''. These data were measured with a DMA as a function of the temperature (ranging from 30 to 425°C) and the loading frequency f (ranging from 0.01 to 150 Hz) [6–8]. The objectives of this research are first to obtain the corresponding master

curves and second to analyze the mechanical relaxations responsible for the viscoelastic behavior of Al–Zn–Mg and Al–Cu–Mg alloys. These alloys feature excellent mechanical properties after proper age hardening and for this reason they are used in a number of industrial applications, especially in the aerospace sector and transport industry. The ageing path, phase transformations, and precipitate types for these alloys have been extensively studied. A summary of this research as reported in the literature can be found in [6–8].

Pure aluminum and aluminum alloys show varied mechanical relaxation phenomena. Namely, Al–Zn alloys may exhibit high internal friction due to large-scale discontinuous precipitation. In particular, the proposed relaxation mechanisms consist of shear stress relaxations across the network of matrix-precipitate interfaces [1]. In contrast with Al–Zn alloys, Al–Cu alloys usually present these phenomena:

(i) A relaxation effect associated with atom groupings within individual clusters [9].

(ii) The Zener peak observed at 173–175°C at 1 Hz in solution treated and quenched samples [1]. This peak declines as Guinier-Preston (GP) II zones precipitate, while it is stable provided that excess vacancies are removed previously (e.g., with a short annealing), since GP-II zones form only if large amounts of quenched-in vacancies are present. Hence, this peak was associated with the alloy with all the Cu in solution. The activation energy E_A of this relaxation is 1.32 ± 0.08 eV/atom (but may change with composition), and the frequency factor k_0 is $10^{15.6\pm1}$ s^{-1}.

(iii) A broad relaxation peak at 135°C associated with θ' phase [1]. The nucleation and growth of θ' particles modify the internal friction behavior in two ways:

(1) It causes the appearance and growth of a peak slightly below the Zener peak temperature. The magnitude of the former peak is approximately proportional to θ' phase fraction. Thus, it declines as θ' phase transforms into θ phase and vanishes completely when no θ' phase is present. This is why it is named θ' peak. For this peak, the width is about 3 times larger than that for a process having a single relaxation time, E_A is 0.95 ± 0.05 eV/atom, and the relaxation time τ_0 is $10^{-12.5\pm0.8}$ s.

(2) It causes a further decline of the Zener peak mentioned above (ultimately, this peak vanishes when θ' phase formation is complete).

(iv) A relaxation peak associated with θ phase [10]. This relaxation has a maximum at 0.1 Hz and disappears after annealing at 550°C. This is why it is associated with θ phase. This relaxation is not thermally activated [11].

Moreover, Al–Zn–Mg and Al–Cu–Mg alloys and pure aluminum may exhibit relaxations associated with dislocations and grain boundaries [12, 13]. Namely, dislocation motion explains some internal friction peaks associated with semicoherent precipitates [14] and the Bordoni peak, which has been extensively studied in cold-worked pure aluminum [1]. Finally, polycrystalline aluminum presents a peak related to grain boundaries at about 300°C at 1 Hz [1]. Some of these and other internal friction mechanisms suggested for aluminum and related metallic materials are explained in [15, 16], like a peak in Al–Mg alloys at 100–200°C also controlled by the Zener mechanism.

The dynamic properties of viscoelastic solids can be described using the complex compliance approach. In this case, for a solid showing a single relaxation process, the real and imaginary parts of the compliance, J_1 and J_2, are given by the Debye equations [1]:

$$J_1(T,\Omega) = J_u + \frac{\delta J}{1+(\Omega\tau)^2}$$
$$J_2(T,\Omega) = \delta J \frac{\Omega\tau}{1+(\Omega\tau)^2}, \quad (1)$$

where $J_u(T)$ is the unrelaxed compliance, $\delta J(T) = J_r - J_u$ is the relaxation of the compliance, $J_r(T)$ is the relaxed compliance, $\Omega = 2\pi f$ is the loading frequency, and $\tau(T)$ is the average mechanical relaxation time of the process/processes occurring at a given temperature. The complex Young's modulus $E = E' + iE''$ is also commonly used to describe the tensile dynamic-mechanical behavior, where

$$E'(T,\Omega) = E'' \frac{J_1}{J_2} \quad (2)$$

$$E''(T,\Omega) = \frac{J_2}{{J_1}^2 + {J_2}^2}. \quad (3)$$

In this case, $E_u(T) = 1/J_u$ is the unrelaxed modulus (i.e., E for $\Omega \to \infty$), $E_r(T) = 1/J_r$ is the relaxed modulus (i.e., E for $\Omega \to 0$), and $\delta E(T) = E_u - E_r$ is the relaxation of the modulus. Indeed, relaxation processes are usually characterized from the analysis of E''. Particularly, E'' peaks (internal friction peaks) are defined by four main characteristics: the intensity (δE) of the peak, its bluntness (or broadness), and the power laws defining the low- and high-frequency tails [17].

The empirical Havriliak–Negami (HN), Cole–Cole (CC), and Cole–Davidson (CD) functions are used to describe the relaxation response in the frequency domain [18]. The HN model is $E(T,\Omega) = E_u[1-(1+(i\Omega\tau)^\alpha)^{-\gamma}]$, where the exponents α and γ describe the broadness of the peak (associated with the distribution of relaxation times) and the asymmetry of the peak, respectively [19]. The CC and CD functions are derived from the HN function; namely, the CC model corresponds to the HN model with $\gamma = 1$ and $0 < \alpha < 1$, while the CD model is the HN model with $\alpha = 1$ and $0 < \gamma < 1$. The CD function can fit asymmetric peaks, with the shape being dictated by γ, while the CC function describes symmetric peaks, with the broadness being dictated by α. The latter parameter, which often increases with temperature, can give information about how distributed are the relaxation times. Classical anelastic relaxations in crystalline metals are restricted to a small volume, for example, defects

Table 1: Mechanical properties of the as-received, commercial aluminum alloys (AA) 7075-T6 and 2024-T3.

Aluminum alloy	Yield stress	UTS	% area reduction	Brinell hardness
AA 7075-T6	502 MPa	583 MPa	12%	HB 161
AA 2024-T3	377 MPa	485 MPa	15%	HB 123

Table 2: Chemical compositions of the as-received, commercial aluminum alloys (AA) 7075-T6 and 2024-T3.

Aluminum alloy	Units	Si	Fe	Cu	Mn	Mg	Zn	Ti	Cr	Al
AA 7075-T6	wt.%	0.06	0.15	1.50	0.01	2.58	6.00	0.05	0.19	89.46
	at.%	0.06	0.08	0.67	0.01	2.99	2.59	0.03	0.10	93.48
AA 2024-T3	wt.%	0.18	0.28	4.46	0.64	1.35	0.04	0.05	0.01	92.98
	at.%	0.18	0.14	1.95	0.32	1.54	0.02	0.03	0.01	95.81

like dislocations and grain boundaries [1]. Accordingly, the relaxations have a much smaller magnitude and the peaks are very close to a Debye relaxation, with $\alpha \approx 1$ and $\gamma \approx 1$ [17].

The distribution of relaxation times can also be related to a spectrum of activation energies. The time-temperature relaxation spectrum $E''(\Omega, T)$ can be modeled by combining a frequency response function (e.g., HN, CD, CC, or other models) with a temperature dependence of the main relaxation time $\tau(T)$, in what is called the TTS principle [4, 5]. In this approach, the shape of $E''(\Omega, T)$ describes the influence of the relaxation time spectrum, that is, the deviation from a Debye process [17]. For the HN, CD, and CC models, the shape is determined by α and/or γ, which are obtained from fitting of the model to the experimental $E''(\Omega, T)$ data. Regarding the temperature dependence of the average or main relaxation time of the process $\tau(T)$, it is often valid to assume an Arrhenius-type temperature dependence for the relaxation rate $1/\tau(T)$ (e.g., when the rate-limiting step of the considered relaxation is that of movement over an energy barrier) [20]:

$$\frac{1}{\tau} = k_0 \exp\left(-\frac{E_A}{k_B T}\right), \tag{4}$$

where $k_0 = 1/\tau_0$ is the frequency factor (or preexponential coefficient), E_A is the activation energy associated with the relaxation, and k_B is the Boltzmann constant. This is why the dynamic response functions may be treated as if they were functions of temperature (while frequency is constant) instead of functions of frequency (while temperature, and thus $\tau(T)$, are constant) [1]. This is the basis of the TTS principle, which establishes the relationship between temperature and time on the relaxation and deformation behavior of viscoelastic materials under constant stress/strain or dynamic loading [4, 5, 21]. For instance, the effect of increasing temperature on the viscoelastic response is similar to reducing frequency.

Accordingly, master curves can be obtained by superimposing the modulus spectra (E' and E'') at different temperatures. This is achieved by shifting horizontally (i.e., along the frequency axis) the isothermal curves of E' and E'' using a shift factor a_T. This factor defines the ratio of relaxation time at a given temperature T to its value at an arbitrary chosen reference temperature T_0 and reflects the segmental or atomic mobility associated with configurational rearrangements in materials [4, 22]. The temperature dependence of a_T has been successfully described by the Williams–Landel–Ferry equation (e.g., for amorphous polymers) [22], the equivalent Vogel–Fulcher–Tammann–Hesse equation, or an Arrhenius-type expression [5]:

$$\ln(a_T) = \frac{E_A}{k_B}\left(\frac{1}{T} - \frac{1}{T_0}\right). \tag{5}$$

A master curve can be used to transform material properties from the frequency domain to the temperature domain, and vice versa [23, 24]. In principle, it allows extrapolating the viscoelastic behavior to any temperature or frequency. However, a master curve associated with a given a_T may only be valid within a limited temperature range, because a_T depends also on ageing (i.e., on the microstructure) and on the relaxation mechanisms of the viscoelastic spectrum. Namely, a_T may exhibit different temperature dependencies from a temperature interval to another (and thus there will be a different master curve in each of these intervals), if phase transformations occur in between or different relaxation mechanisms intervene. This can be used to detect the occurrence of transformations or changes in the dominant relaxation mechanisms based on DMA data, while E_A in (5) gives useful information on the mechanical relaxation processes [5].

2. Materials and Methods

The specimens were prepared from sheet of commercial aluminum alloys (AA) 7075-T6 and 2024-T3. The T6 temper consists in solution heat-treatment at 480°C for 1 h, followed by rapid water quenching to room temperature (RT) and artificial ageing at 120°C for 24 h. The T3 temper consists in solution heat-treatment at 480°C for 1 h, followed by rapid water quenching to RT, cold-working, and natural ageing. Tables 1 and 2 show, respectively, the mechanical properties and compositions in wt.% and at.% for AA 7075-T6 and 2024-T3, as provided by the supplier (Alu-Stock, SA). A first set of specimens was machine cut from the as-received alloys to rectangular plates 60 mm long, 10 mm wide, and 2 mm thick. A second set of identical plates was solution treated at 477°C for

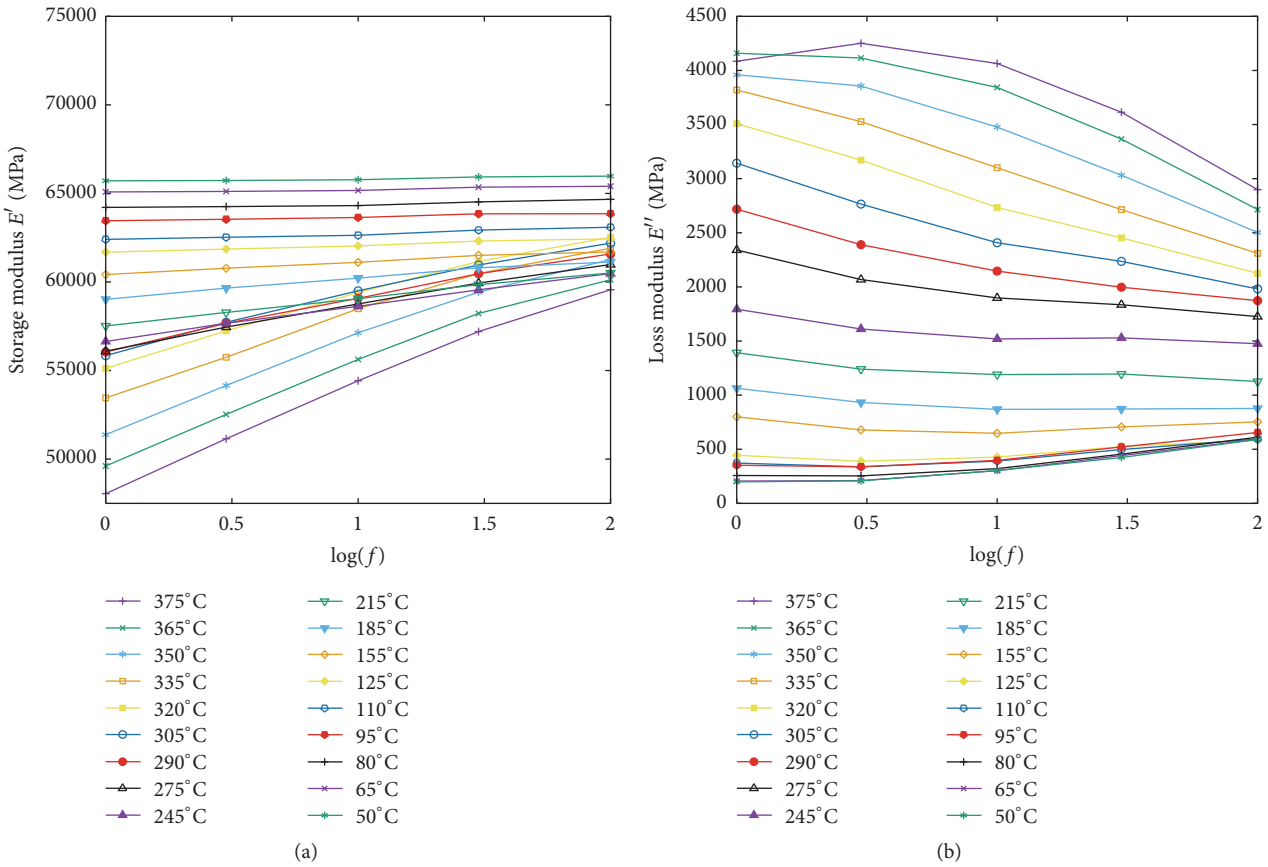

FIGURE 1: Isothermal storage modulus E' (a) and loss modulus E'' (b) versus logarithm of the frequency f from DMA tests on AA 7075-T6 at frequencies ranging from 1 to 100 Hz and from 50 to 375°C.

30 min to remove the T6 temper, rapidly quenched in water to RT and tested immediately after. A TA Instruments Q800 DMA was used to measure the viscoelastic response of the studied materials (i.e., E' and E''; more details can be found in [6–8]) in N_2 atmosphere. The 3-point bending clamp was used, with length between unmovable supports of 50 mm and preload force of 0.10 N, and the DMA was set to sequentially apply dynamic loading with frequencies ranging from 0.01 to 150 Hz, at temperatures from 30 to 425°C in step increments of 5°C.

3. Results and Discussion

3.1. Experimental Results for E' and E''. Figures 1(a) and 1(b) show, respectively, isothermal curves of E' and E'' versus frequency obtained from DMA experiments for AA 7075-T6 at various temperatures, while Figures 2(a) and 2(b) show the same curves for solution treated AA 7075.

Figures 3(a) and 3(b) show, respectively, isothermal curves of E' and E'' versus frequency obtained from DMA experiments for AA 2024-T3 at various temperatures, while Figures 4(a) and 4(b) show the same curves for solution treated AA 2024.

The results confirm that the viscoelastic response of the studied alloys depends on the temperature and the loading frequency. The larger decrease (increase) of E' (E'') with temperature observed for lower frequencies (see Figures 1–4) is due to the Arrhenius-type behavior of the relaxation rate, where the mechanical relaxation time diminishes as temperature increases [1]. The decrease of E' with temperature (observed as early as at RT) is explained by the dependence of the elastic moduli on temperature, a well-known phenomenon for metals, for example, for the static elastic moduli of pure aluminum and AA 2024 [25–27] and for the dynamic elastic moduli of pure aluminum and AA 6061 reinforced with Al_2O_3 [28]. As shown also in Figures 1–4, E' and E'' depend more significantly on the frequency at higher temperatures. This is also explained by the Arrhenius-type behavior of the relaxation rate [6–8].

3.2. Master Curves for E' and E''. The isothermal curves shown in Figures 1–4, as obtained from the DMA data, were superimposed by shifting along the frequency axis using an Arrhenius-type shift factor a_T ((5)) [5]. The arbitrary chosen reference temperature T_0 was 215°C. Using this approach, that is, applying the TTS principle, it was possible to identify a master curve for E' in a low-temperature region, as shown in Figure 5 for AA 7075-T6 and 7075, and in Figure 7 for AA 2024-T3 and 2024. Also, for all the studied alloys, it was possible to identify master curves for both E' and E'' in a high-temperature region, as shown in Figure 6 for AA 7075-T6 and

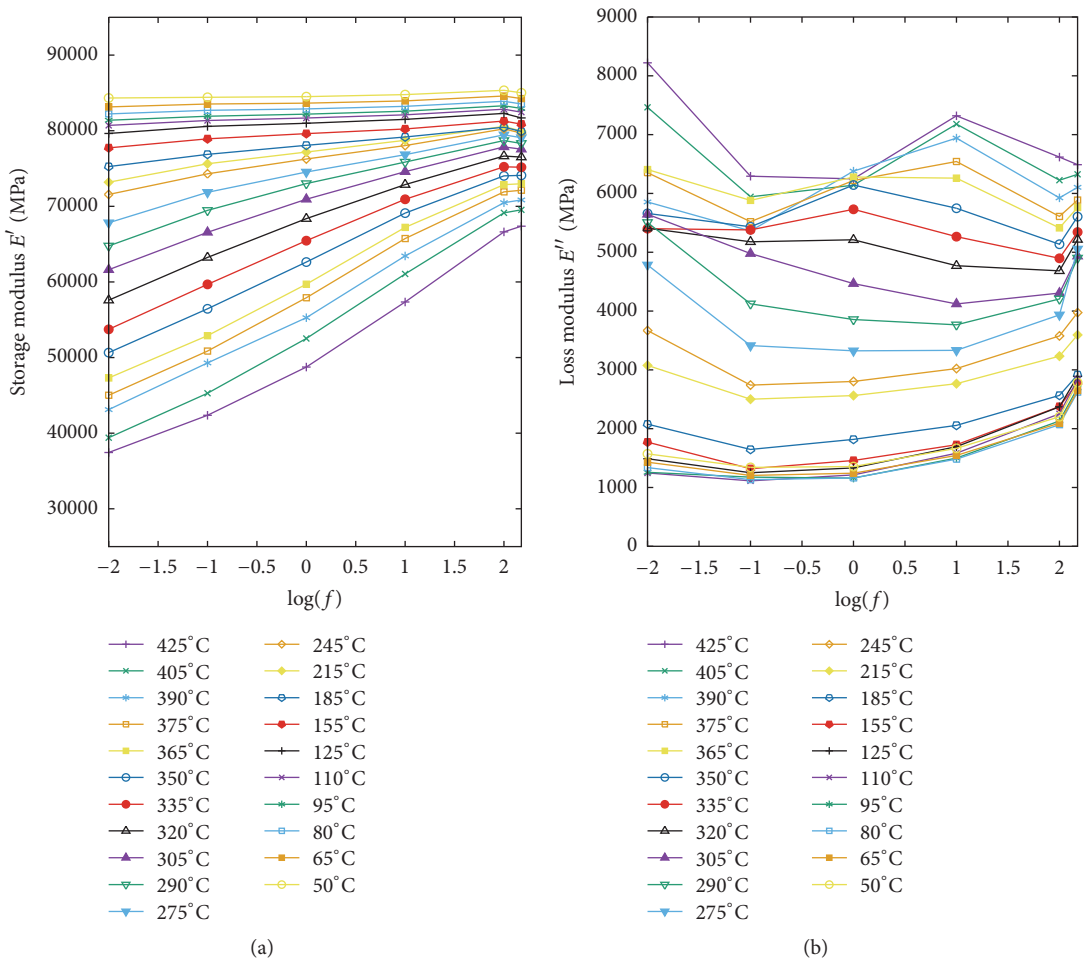

FIGURE 2: Isothermal storage modulus E' (a) and loss modulus E'' (b) versus logarithm of the frequency f from DMA tests on solution treated AA 7075 at frequencies ranging from 0.01 to 150 Hz and from 50 to 425°C.

7075, and in Figure 8 for AA 2024-T3 and 2024. These temperature regions, coincidental with the stable intervals where no phase transformations occur, can also be observed in DSC thermograms (see Tables 3 and 4 in [7]). The low-temperature stable region ranges approximately from RT to 150°C, which is reasonable assuming that formation of GP zones and/or Guinier-Preston-Bagariastkij (GPB) zones is already complete in our samples prior to testing (this is justified in [7]) and that dissolution of GP zones and GPB zones has not begun. Only the high-frequency data at 50, 65, 80, and 95°C for solution treated AA 7075 seems to fall a bit far from the master curve, suggesting that maybe a different type of relaxation is playing an important role in these cases or that GP zones formation was still not completed for this alloy at these temperatures. The high-temperature stable region ranges approximately from 320 to 375°C, before the onset of the dissolution of equilibrium phases. It was not possible to obtain any master curve for E' and E'' between 150 and 300°C or to superpose these data in any of the master curves mentioned above. The reason is that this is not a stable temperature interval, that is, it is overlapped by on-going transformations like dissolution of GP zones and/or GPB zones and precipitation of metastable and equilibrium phases. The activation energies used in (5) to obtain the master curves shown in Figures 5–8 were established by empirical fit (see Tables 3 and 4).

The absolute values of E' and E'' measured by the DMA may differ noticeably from one test to another (e.g., due to instrument error, imperfections of the samples, or errors in measuring their dimensions). That is why no attempt is made to provide microstructural explanations for the differences observed between the studied alloys in, for instance, the absolute values of E', as shown in Figures 5 and 7. Namely, these differences fall within instrument error.

The different temperature dependencies of a_T for the identified master curves (manifested by different values of E_A in the Arrhenius expression for a_T, with E_A being smaller for the low-temperature region compared to the high-temperature region) are due, on the one hand, to the occurrence of microstructural changes between the mentioned temperature regions associated with the phase transformations mentioned above. On the other hand, the differences are also caused by the different relaxation mechanisms acting in one region with respect to the other (the relaxation mechanisms change as the material changes). Hence, from the TTS

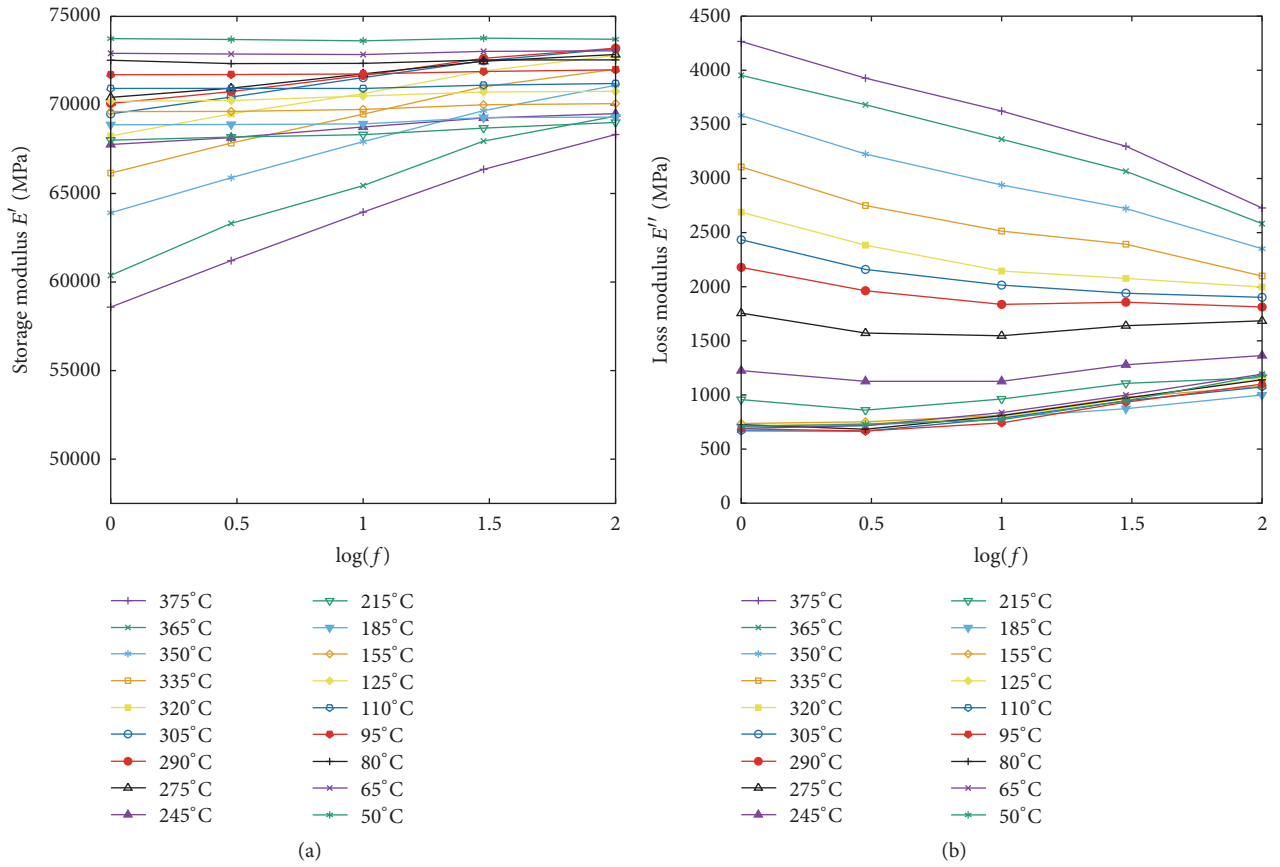

Figure 3: Isothermal storage modulus E' (a) and loss modulus E'' (b) versus logarithm of the frequency f from DMA tests on AA 2024-T3 at frequencies ranging from 1 to 100 Hz and from 50 to 375°C.

Table 3: Activation energy E_A in the Arrhenius-type equation for the shift factor a_T for Al–Zn–Mg alloys.

Temperature region	E_A in Arrhenius-type equation for a_T	
	From E' data [eV/atom]	From E'' data [eV/atom]
Low temperature (AA 7075-T6)	0.30	No master curve was obtained[a]
High temperature (AA 7075-T6)	0.60	0.60
Low temperature (AA 7075)	0.30	No master curve was obtained[a]
High temperature (AA 7075)	0.60	0.60

[a]Only values of activation energy below 0.01 eV/atom (with little physical significance) resulted in an acceptable degree of superposition of E'' curves. Therefore, this result was disregarded.

Table 4: Activation energy E_A in the Arrhenius-type equation for the shift factor a_T for Al–Cu–Mg alloys.

Temperature region	E_A in Arrhenius-type equation for a_T	
	From E' data [eV/atom]	From E'' data [eV/atom]
Low temperature (AA 2024-T3)	0.30	No master curve was obtained[a]
High temperature (AA 2024-T3)	0.80	0.80
Low temperature (AA 2024)	0.30	No master curve was obtained[a]
High temperature (AA 2024)	0.80	0.80

[a]Only values of activation energy below 0.01 eV/atom (with little physical significance) resulted in an acceptable degree of superposition of E'' curves. Therefore, this result was disregarded.

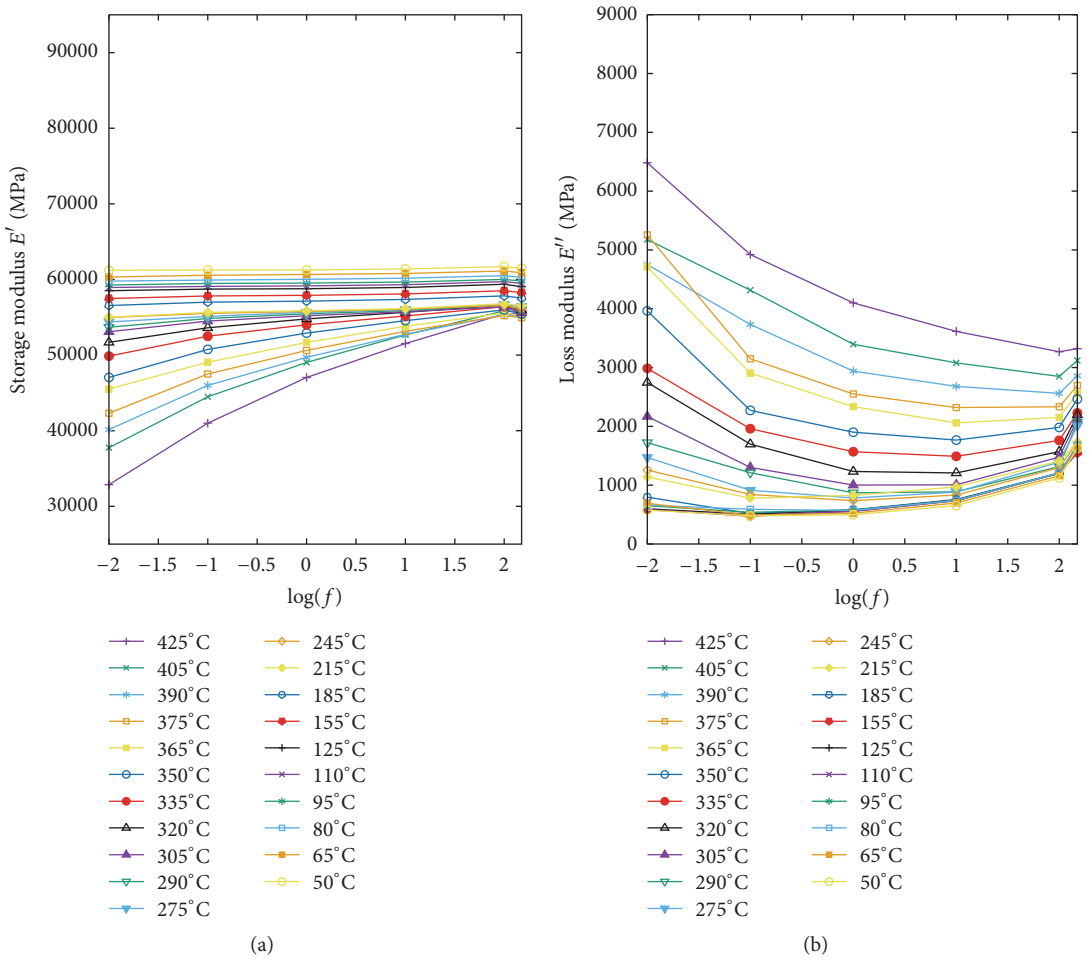

Figure 4: Isothermal storage modulus E' (a) and loss modulus E'' (b) versus logarithm of the frequency f from DMA tests on solution treated AA 2024 at frequencies ranging from 0.01 to 150 Hz and from 50 to 425°C.

Table 5: Characteristic parameters of the Debye peaks in Figure 9(a), associated with a hypothetical mechanical relaxation. The values of E_u and E_r were fitted empirically. Only τ at 375°C was fitted empirically, while τ at 350 and 365°C was obtained with an Arrhenius equation for $1/\tau$ ((4)) with activation energy 0.60 eV/at.

Temperature	τ [s]	E_u [GPa]	E_r [GPa]	J_u [GPa^{-1}]	δJ [GPa^{-1}]
375°C	0.50	61.5	53.6	1.63×10^{-2}	2.40×10^{-3}
365°C	0.59	64.5	56.9	1.55×10^{-2}	2.07×10^{-3}
350°C	0.77	65.3	57.9	1.53×10^{-2}	1.95×10^{-3}

results it appears that phase transformations have also an influence on E' and E'', as suggested previously [1, 7, 29].

3.3. Analysis of the Measured E'' Peaks. For AA 7075-T6, the isothermal E'' curves at 350, 365, and 375°C show a peak at around 3 Hz, as shown in Figure 1(b). For AA 7075, this peak shifts from 1 to 10 Hz as temperature rises from 320 to 425°C as shown in Figure 2(b). Figure 9(a) shows Debye peaks superimposed to the isothermal E'' curves of AA 7075-T6 at 350, 365, and 375°C. The Debye peaks correspond to a hypothetical mechanical relaxation with characteristic parameters as given in Table 5. The values of E_u and E_r in Table 5 were fitted empirically bearing in mind that (1) from the results in Figure 1(b), E_u and E_r should be around 60 and 50 GPa, respectively; (2) $E_u > E_r$, since materials exhibit a stiffer response at higher frequencies; and (3) E_u and E_r decrease with temperature, as usual for elastic moduli of metals [25–27]. Since the values of τ at the various temperatures are linked by (4) (the activation energy being 0.60 eV/atom, from the results in Table 3), only the value of τ at 375°C was fitted empirically. The purpose of this rough fitting was not to compute the best fit values for those parameters (then this procedure would not be the most appropriate) but simply to show that since the measured E''

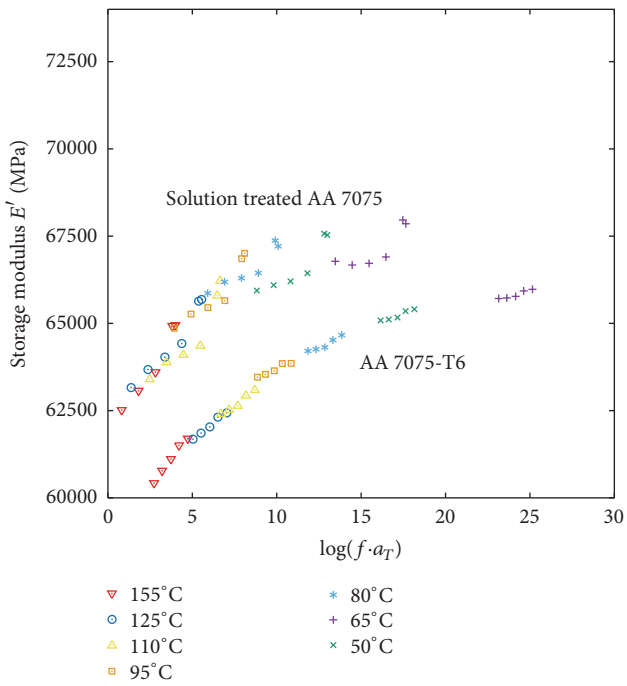

Figure 5: Master curve showing the storage modulus E' versus the logarithm of the frequency f times the shift factor a_T. These curves resulted from horizontal shifting of the isothermal E' curves from DMA tests on AA 7075-T6 and solution treated AA 7075, at temperatures from 50 to 155°C.

peaks are much broader than the Debye peak, they do not correspond to a single relaxation, but to several overlapping or coupled relaxations or to a single mechanism with a distribution of relaxation times. The results in Figure 9(b) also suggest that the measured viscoelastic response may be associated with more than one mechanical relaxation process. Particularly, the value of δE, as obtained from the Debye equation corresponding to a single relaxation, is smaller than the magnitude of the relaxation of E' that can be inferred from E'' results in the limited test frequency range.

For one test on AA 2024-T3, an inflexion is observed centered around 1 Hz for 365 to 425°C, and peaks are observed at around 100 Hz for 100 to 160°C. However, for most tests on AA 2024-T3 and 2024, no E'' peak can be observed in the studied frequency and temperature ranges. For example, the Zener peak often present in solution treated and quenched Al–Cu alloys at 173–175°C and 1 Hz [1] is not observed in our results. If for AA 2024 (which was solution treated and quenched) the peak is not present, this may be due to (1) presence of GP-II zones, (2) the effect of the other elements present in this alloy aside from Cu, (3) the formation of phase θ', causing a decline of the Zener peak, which may eventually vanish when θ' phase formation is complete [1], or, (4) most likely, the Cu content in the studied alloys being so low that there are not enough Cu atomic pairs for this Zener peak to become visible (for instance, Golovin et al. [15] did not distinguish a Zener peak in Al–Mg alloys due to reorientation of Mg–Mg atom pairs in the aluminum solid solution for alloys with Mg content below 5 wt.%). In most of

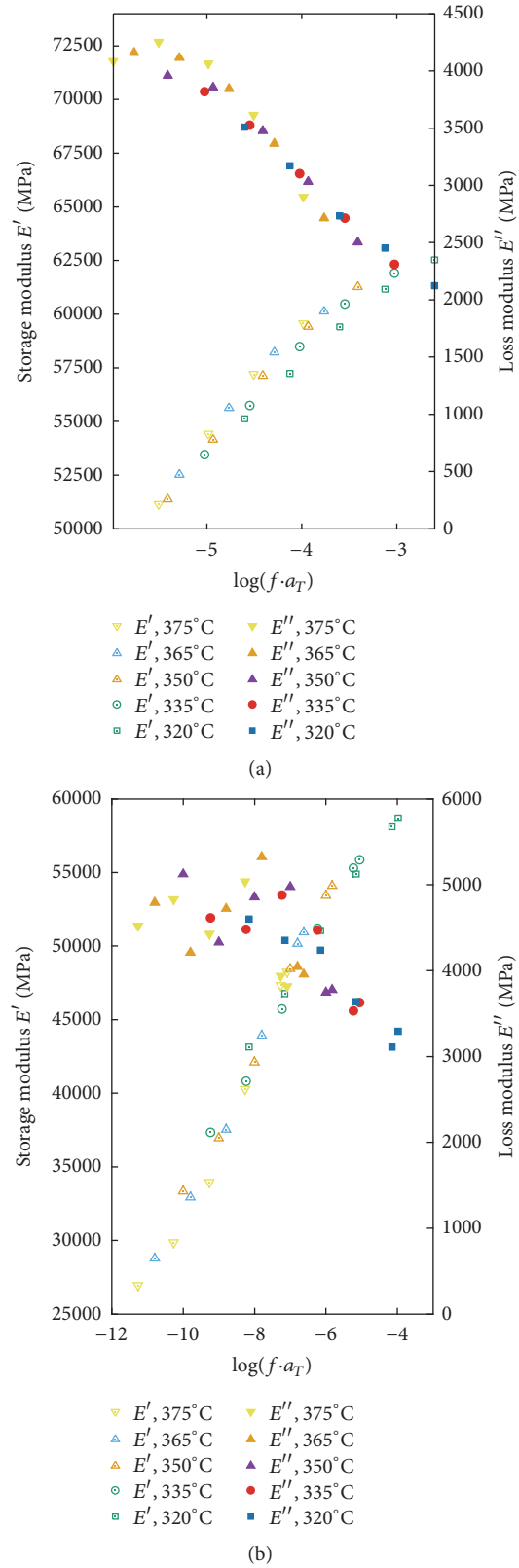

Figure 6: Master curves showing the storage modulus E' (hollow symbols) and the loss modulus E'' (solid-fill symbols) versus the logarithm of the frequency f times the shift factor a_T. These curves resulted from horizontal shifting of the isothermal curves of E' and E'' from DMA tests on AA 7075-T6 (a) and solution treated AA 7075 (b), from 320 to 375°C.

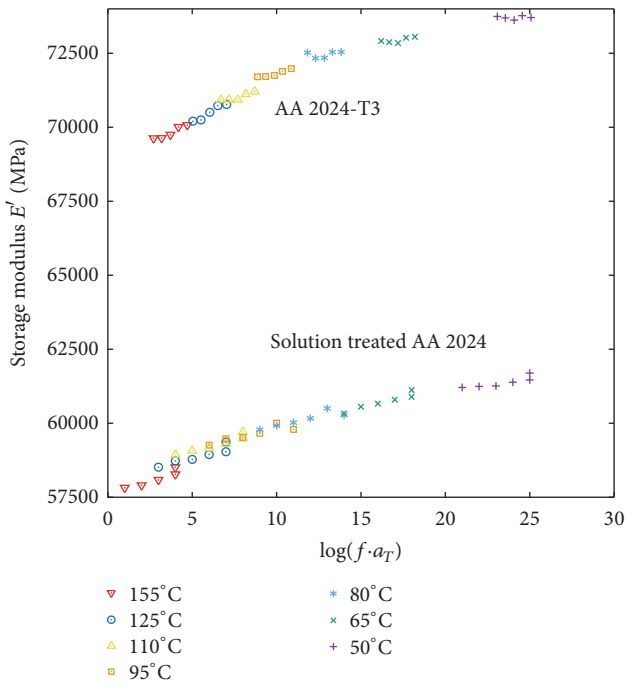

FIGURE 7: Master curve showing the storage modulus E' versus the logarithm of the frequency f times the shift factor a_T. These curves resulted from horizontal shifting of the isothermal E' curves from DMA tests on AA 2024-T3 and solution treated AA 2024, at temperatures from 50 to 155°C.

our results (see Figure 2 in [7]), we can hardly distinguish the broad relaxation peak (three times broader than the Debye peak) at 135°C, associated with θ' phase, with magnitude proportional to θ' phase fraction [1].

For the studied alloys, the results show monotonical growth of E'' with temperature above 200°C (see, for instance, Figure 2 in [6] and Figure 2 in [7], resp.). This is usually explained by presence of coupled or overlapping relaxations [1, 15] and by the high-temperature internal friction background, which is roughly exponential with temperature for most materials [15, 16]. This background is linked to thermally activated viscous deformation, mainly associated with diffusion-controlled dislocation motion. A relaxation probably contributing to this growth of E'' is the internal friction peak typically exhibited by polycrystalline aluminum centered at ≈300°C. This peak is traditionally associated with grain boundary sliding (GBS) [1, 15, 16] and has been observed also in Al–Mg, Al–Zn–Mg, and Al–Cu–Mg alloys [12, 13]. For AA 2024-T3 and 2024, a relaxation peak associated with θ phase [10] is also probably contributing to the monotonical growth of E''. Finally, there is also a contribution by the linear thermoelastic background, which is proportional to temperature, but it should not be very significant in the studied frequency range [16].

For the studied alloys in the considered ranges, it is difficult to ascertain whether any E'' peak is fully captured (i.e., whether the results capture both tails of the peak). Hence, it is not convenient to use the HN model or CD model to analyze the results, because it is difficult to establish whether the peaks are asymmetric or not. An alternative to obtain information from the relaxation process (or processes) responsible for those peaks is to analyze the observed tails of the peaks [17, 18]. For a given value of $\Omega\tau$, it can be derived from (1) and (3) that the value of E'' is the same no matter the frequency. Hence, for each of the curves corresponding to a different frequency in Figure 2 in [7], we obtained the temperature for a same value of E'' (i.e., a same value of $\Omega\tau$). With these data, an Arrhenius plot can be obtained following (4), showing the logarithm of the frequency versus the reciprocal of the temperature, where $\ln(\Omega) = \ln(\Omega\tau) - \ln(\tau_0) - E_A/k_BT$ (see Figure 10). Since the value of $\Omega\tau$ is known, from the Arrhenius plot it is possible to estimate E_A and τ_0.

Using this procedure for four different values of E'' for each alloy (1980, 2000, 2020, and 2040 MPa for AA 7075-T6 and 1280, 1300, 1320, and 1340 MPa for AA 2024-T3), the apparent activation parameters were obtained for the monotonical growth region of E''. The differences in the computed activation energy for the four cases with respect to the average are below 1.5% for AA 7075 and 4.3% for AA 2024. This proves the robustness of the method and the precision and high-confidence of the activation energy results. Particularly, the apparent activation parameters, which may correspond to superposed tails of coupled or overlapped peaks, are $E_A = 1.50 \pm 0.01$ eV/atom and $\tau_0 = (1.44 \pm 0.40) \times 10^{-15}$ s for AA 7075-T6 and $E_A = 1.83 \pm 0.05$ eV/atom and $\tau_0 = (1.45 \pm 1.40) \times 10^{-17}$ s for AA 2024-T3. These values suggest that the relaxations may correspond effectively to GBS [1, 15]. For example, the relaxation times are far from those typical of relaxations caused by dislocations (for which τ_0 usually ranges from 10^{-10} to 10^{-13}) [15], while the activation energies are close to 1.48 eV/atom, as reported for GBS [1, 15].

The higher value of E_A for AA 2024-T3 indicates that, for given conditions, it is more difficult and less frequent for GBS to proceed in this alloy compared to AA 7075-T6. Since GBS has a significant influence on creep at high stress values, for example, in the beginning of the tertiary creep acceleration [30], this would be consistent with the creep response of Al–Cu–Mg alloys, which is superior to Al–Zn–Mg alloys in the tertiary stage; see, for instance, a comparison of the creep behavior of AA 2419 at 340 MPa and 100°C [31] with that of AA7010 at 350 MPa and 100°C [30]. AA 7010 has higher minimum creep strain rate and has lower time to fracture (718000 versus 838000 s) and shows higher creep strain at fracture. Moreover, since fatigue is a consequence of microstructural changes that must have also an effect on the viscoelastic response [2], if GBS contributes also to fatigue problems, the higher value of E_A for the relaxation associated with GBS in Al–Cu–Mg alloys is also consistent with the better fatigue response of these alloys compared to Al–Zn–Mg alloys.

4. Conclusions

The main conclusions of this investigation are summarized as follows:

(1) The TTS principle, which has not been applied to crystalline materials before, was successfully applied to the viscoelastic response of commercial AA 7075

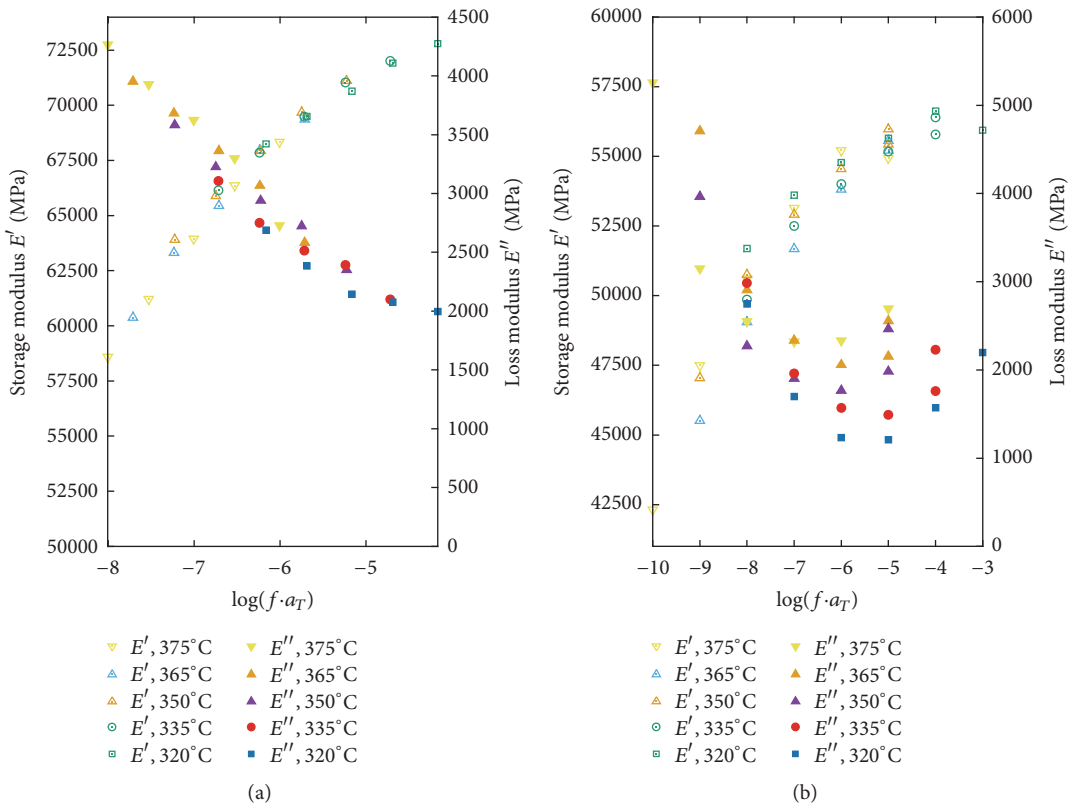

FIGURE 8: Master curves showing the storage modulus E' (hollow symbols) and the loss modulus E'' (solid-fill symbols) versus the logarithm of the frequency f times the shift factor a_T. These curves resulted from horizontal shifting of the isothermal curves of E' and E'' from DMA tests on AA 2024-T3 (a) and solution treated AA 2024 (b), from 320 to 375°C.

and 2024. Master curves were obtained for E' at low temperatures (from RT to 150°C) and for both E' and E'' at high temperatures (from 320 to 375°C). Both the low- and high-temperature ranges are coincidental with stable intervals where no reactions occur. This enables extrapolation of the viscoelastic data to any frequency and temperature within the range of validity of the master curve.

(2) The different temperature dependencies of the shift factors for the identified master curves, manifested by different activation energies in the Arrhenius expressions for the shift factor, are due to the occurrence of microstructural changes and variations in the relaxation mechanisms between the mentioned temperature ranges.

(3) E'' peaks with frequency observed for Al–Zn–Mg alloys are broader than the Debye peak. Thus, they correspond to several overlapping or coupled relaxations, or to a single mechanism with a distribution of relaxation times.

(4) For most of our tests on Al–Cu–Mg alloys, no E'' peak with frequency can be observed. In particular, the Zener peak often present in solution treated and quenched Al–Cu alloys, as well as a peak in Al–Mg alloys at 100–200°C also controlled by the Zener mechanism, is not observed. The most likely explanation is that the Cu and Mg content of these alloys are so low that there are not enough Cu or Mg atomic pairs for this Zener peaks to become visible.

(5) For all the studied alloys, E'' grows monotonically with temperature above 200°C. This fact is explained by the presence of coupled or overlapping relaxations (e.g., internal friction associated with GBS and intermediate and/or equilibrium precipitates) and by the high-temperature internal friction background.

(6) From the analysis of the tails of these coupled or overlapped peaks, the apparent activation parameters obtained with high-confidence are as follows: $E_A = 1.50 \pm 0.01$ eV/atom and $\tau_0 = (1.44 \pm 0.40) \times 10^{-15}$ s for AA 7075-T6 and $E_A = 1.83 \pm 0.05$ eV/atom and $\tau_0 = (1.45 \pm 1.40) \times 10^{-17}$ s for AA 2024-T3, corresponding to typical values of relaxations associated with GBS. The higher value of E_A for AA 2024-T3 indicates that, for given conditions, it is more difficult and less frequent for GBS to proceed in this alloy compared to AA 7075-T6. Since GBS has a significant effect on tertiary creep acceleration, this would be consistent with the creep response of Al–Cu–Mg alloys, which is superior to Al–Zn–Mg alloys in the tertiary stage.

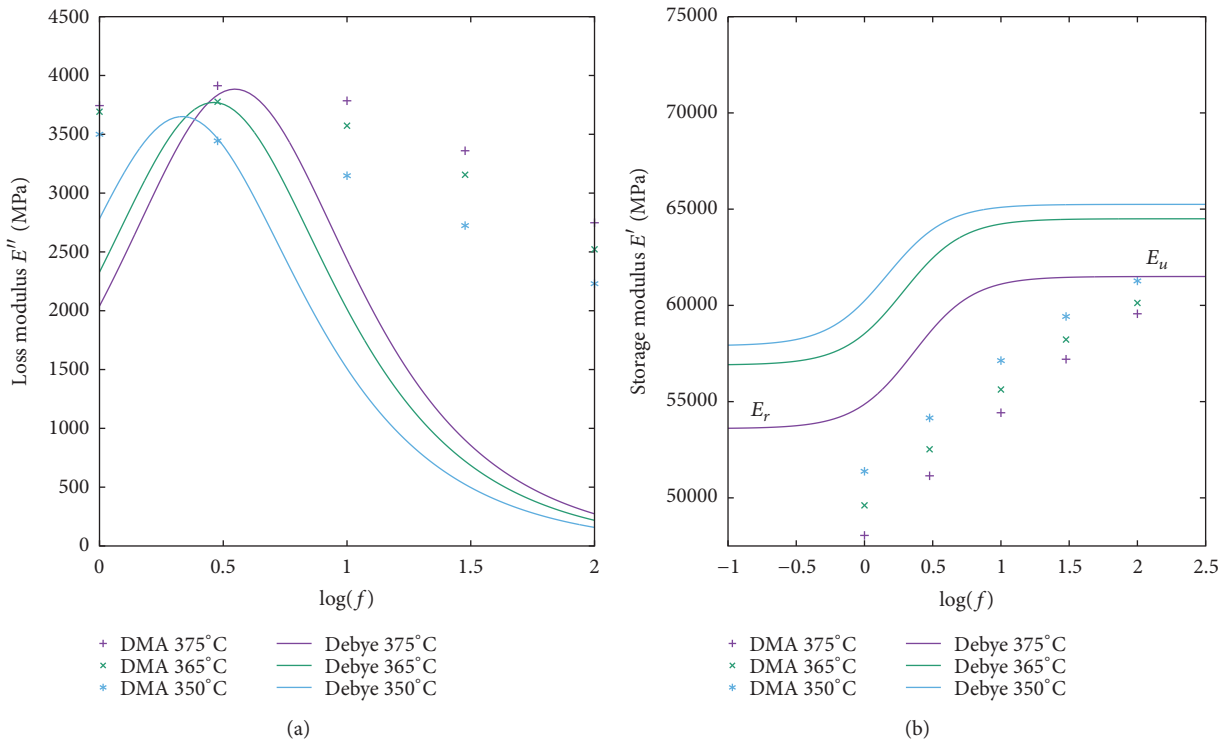

Figure 9: From DMA tests on AA 7075-T6 at 350, 365, and 375°C: isothermal loss modulus E'' versus logarithm of the frequency f and Debye peaks as given by Debye equation (a); and storage modulus E' versus logarithm of the frequency f as given by Debye equation (b). E_u and E_r are the unrelaxed and relaxed dynamic Young's moduli, respectively.

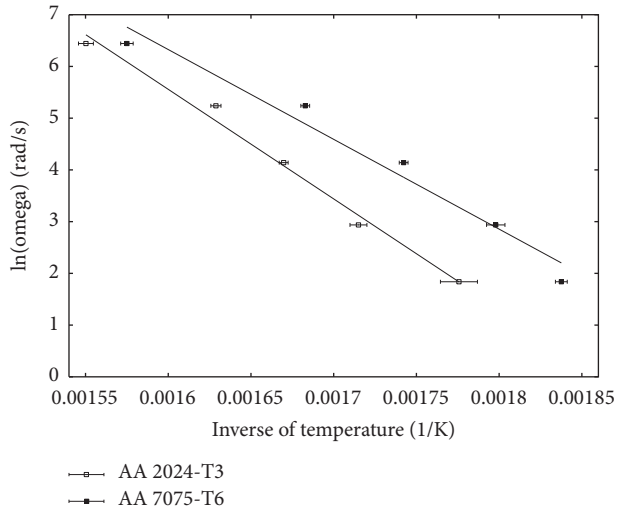

Figure 10: Arrhenius plots showing the logarithm of the frequency versus the reciprocal of the temperature for the tails of the peaks observed for AA 7075-T6 and 2024-T3 at high temperatures.

(7) The proposed approach allows relating phase transformations to the viscoelastic properties and mechanical relaxations of the studied alloys, by comparing the values of E_A derived from the master curves and the analysis of the internal friction peaks, with values of E_A attributed to particular relaxations in the literature.

(8) The DMA, besides allowing for mechanical spectroscopy, is also an adequate tool for having insight into the microstructure and phase transformations. Moreover, contrary to DSC analysis, the dynamic-mechanical response is independent of the total enthalpy change of the reactions, thus allowing for the analysis of transformations involving minority phases.

Conflicts of Interest

The authors declare that they have no conflicts of interest regarding the publication of this paper.

Acknowledgments

This work is supported by the MINECO Grant FIS2014-54734-P and the Generalitat de Catalunya-AGAUR Grant 2014 SGR 00581. The authors thank also Dr. Eloi Pineda for the valuable help.

References

[1] A. S. Nowick and B. S. Berry, *Anelastic Relaxation in Crystalline Solids*, Academic Press, New York, NY, USA, 1972.

[2] A. Puskar and S. A. Golovin, *Fatigue in Materials: Cumulative Damage Processes*, Elsevier Science Ltd, Amsterdam, The Netherlands, 1985.

[3] Y. M. Soifer, N. P. Kobelev, I. G. Brodova, A. N. Manukhin, E. Korin, and L. Soifer, "Internal friction and the young's modulus change associated with amorphous to nanocrystalline phase transition in Mg-Ni-Y alloy," *Nanostructured Materials*, vol. 12, no. 5, pp. 875–878, 1999.

[4] H. Jeong, J. Kim, W. Kim, and D. Kim, "The mechanical relaxations of a Mm55Al25Ni10Cu10 amorphous alloy studied by dynamic mechanical analysis," *Materials Science and Engineering: A*, vol. 385, no. 1-2, pp. 182–186, 2004.

[5] H. T. Jeong, E. Fleury, W. T. Kim, D. H. Kim, and K. Hono, "Study on the mechanical relaxations of a Zr36Ti24Be40 amorphous alloy by time-temperature superposition principle," *Journal of the Physical Society of Japan*, vol. 73, no. 11, pp. 3192–3197, 2004.

[6] J. I. Rojas, A. Aguiar, and D. Crespo, "Effect of temperature and frequency of dynamic loading in the viscoelastic properties of aluminium alloy 7075-T6," *Physica Status Solidi (C) Current Topics in Solid State Physics*, vol. 8, no. 11-12, pp. 3111–3114, 2011.

[7] J. I. Rojas and D. Crespo, "Modeling of the effect of temperature, frequency, and phase transformations on the viscoelastic properties of AA 7075-T6 and AA 2024-T3 aluminum alloys," *Metallurgical and Materials Transactions A: Physical Metallurgy and Materials Science*, vol. 43, no. 12, pp. 4633–4646, 2012.

[8] J. I. Rojas, *Microstructural Characterization & Viscoelastic Properties of AlZnMg & AlCuMg Alloys*, Universitat Politècnica de Catalunya, 2012.

[9] K. J. Williams and K. M. Entwistle, "The damping of quench-ageing duralumin vibrating at about 1 cycle per second," *Journal of the Institute of Metals*, vol. 87, no. 5, pp. 141–144, 1959.

[10] P. Cui and T. Kê(Ge Tingsui), "Anelastic relaxation peak associated with the presence of incoherent θ phase in Al-4wt.%Cu alloy," *Materials Science and Engineering: A*, vol. 150, no. 2, pp. 281–288, 1992.

[11] A. Rivière and V. Pelosin, "Low frequency relaxation effect observed on 2024 aluminum alloy," *Journal of Alloys and Compounds*, vol. 310, no. 1-2, pp. 173–175, 2000.

[12] S. Belhas, A. Riviere, J. Woirgard, J. Vergnol, and J. De Fouquet, "High temperature relaxation mechanisms in cu-al solid solutions," *Le Journal de Physique Colloques*, vol. 46, no. C10, pp. C10-367–C10-370, 1985.

[13] A. Rivière, M. Gerland, and V. Pelosin, "Influence of dislocation networks on the relaxation peaks at intermediate temperature in pure metals and metallic alloys," *Materials Science and Engineering A*, vol. 521-522, pp. 94–97, 2009.

[14] M. Mondino and G. Schoeck, "Coherency loss and internal friction," *Physica Status Solidi (A)*, vol. 6, no. 2, pp. 665–670, 1971.

[15] I. S. Golovin, A. V. Mikhaylovskaya, and H.-R. Sinning, "Role of the β-phase in grain boundary and dislocation anelasticity in binary Al-Mg alloys," *Journal of Alloys and Compounds*, vol. 577, pp. 622–632, 2013.

[16] M. Yamaguchi, J. Bernhardt, K. Faerstein et al., "Fabrication and characteristics of melt-spun Al ribbons reinforced with nano/micro-BN phases," *Acta Materialia*, vol. 61, no. 20, pp. 7604–7615, 2013.

[17] C. Liu, E. Pineda, and D. Crespo, "Mechanical relaxation of metallic glasses: an overview of experimental data and theoretical models," *Metals*, vol. 5, no. 2, pp. 1073–1111, 2015.

[18] E. Pineda, P. Bruna, B. Ruta, M. Gonzalez-Silveira, and D. Crespo, "Relaxation of rapidly quenched metallic glasses: effect of the relaxation state on the slow low temperature dynamics," *Acta Materialia*, vol. 61, no. 8, pp. 3002–3011, 2013.

[19] K. L. Ngai, *Relaxation and Diffusion in Complex Systems*, Partially Ordered Systems, Springer, New York, NY, USA, 1st edition, 2011.

[20] D. Suh and R. H. Dauskardt, "Mechanical relaxation time scales in a Zr-Ti-Ni-Cu-Be bulk metallic glass," *Journal of Materials Research*, vol. 17, no. 6, pp. 1254–1257, 2002.

[21] M. Zink, K. Samwer, W. L. Johnson, and S. G. Mayr, "Validity of temperature and time equivalence in metallic glasses during shear deformation," *Physical Review B—Condensed Matter and Materials Physics*, vol. 74, no. 1, Article ID 012201, 2006.

[22] M. L. Williams, R. F. Landel, and J. D. Ferry, "The temperature dependence of relaxation mechanisms in amorphous polymers and other glass-forming liquids," *Journal of the American Chemical Society*, vol. 77, no. 14, pp. 3701–3707, 1955.

[23] M. D. Rao, "Recent applications of viscoelastic damping for noise control in automobiles and commercial airplanes," *Journal of Sound and Vibration*, vol. 262, no. 3, pp. 457–474, 2003.

[24] D. I. G. Jones, "On temperature-frequency analysis of polymer dynamic mechanical behaviour," *Journal of Sound and Vibration*, vol. 140, no. 1, pp. 85–102, 1990.

[25] G. N. Kamm and G. A. Alers, "Low-temperature elastic moduli of aluminum," *Journal of Applied Physics*, vol. 35, no. 2, pp. 327–330, 1964.

[26] J. A. Brammer and C. M. Percival, "Elevated-temperature elastic moduli of 2024 aluminum obtained by a laser-pulse technique—elastic moduli for a structural aluminum are determined in the temperature range of 22◦ to 500◦C from measurements of elastic waves generated in slender rods by the deposition of laser energy pulses," *Experimental Mechanics*, vol. 10, no. 6, pp. 245–250, 1970.

[27] P. M. Sutton, "The variation of the elastic constants of crystalline aluminum with temperature between 63°K and 773°K," *Physical Review*, vol. 91, no. 4, pp. 816–821, 1953.

[28] A. Wolfenden and J. M. Wolla, "Mechanical damping and dynamic modulus measurements in alumina and tungsten fibre-reinforced aluminium composites," *Journal of Materials Science*, vol. 24, no. 9, pp. 3205–3212, 1989.

[29] T. Das, S. Bandyopadhyay, and S. Blairs, "DSC and DMA studies of participate reinforced metal matrix composites," *Journal of Materials Science*, vol. 29, no. 21, pp. 5680–5688, 1994.

[30] H. Burt and B. Wilshire, "Theoretical and practical implications of creep curve shape analyses for 7010 and 7075," *Metallurgical and Materials Transactions A*, vol. 37, no. 12, pp. 1005–1015, 2006.

[31] H. Burt and B. Wilshire, "Theoretical and pratical implications of creep curve shape analyses for 2124 and 2419," *Metallurgical and Materials Transactions A: Physical Metallurgy and Materials Science*, vol. 35, no. 6, pp. 1691–1701, 2004.